Electron transfer in Me-blocked heterodimeric α,γ-peptide nanotubular donor–acceptor hybrids

Roberto J. Brea*, Luis Castedo*, Juan R. Granja*†, M. Ángeles Herranz‡, Luis Sánchez‡, Nazario Martín†‡, Wolfgang Seitz§, and Dirk M. Guldi†§

*Departamento de Química Orgánica, Facultad de Química, Universidad de Santiago, E-15782 Santiago de Compostela, Spain; ‡Departamento de Química Orgánica, Facultad de Ciencias Químicas, Universidad Complutense, E-28040 Madrid, Spain; and §Institute of Physical and Theoretical Chemistry, Interdisciplinary Center for Molecular Materials, Egerlandstrasse 3, 91058 Erlangen, Germany

Edited by Harry B. Gray, California Institute of Technology, Pasadena, CA, and approved January 22, 2007 (received for review October 26, 2006)

Bio-inspired cyclopeptidic heterodimers built on β-sheet-like hydrogen-bonding networks and bearing photoactive and electroactive chromophores on the outer surface have been prepared. Different cross-strand pairwise relationships between the side chains of the cyclic α,γ-peptides afford the heterodimers as three nonequivalent dimeric species. Steady-state and time-resolved spectroscopies clearly show an electron transfer process from π-extended tetrathiafulvalene, covalently attached to one of the cyclopeptides, to photoexcited [60]fullerene, located on the complementary cyclopeptide. The charge-separated state was stabilized for up to 1 μs before recombining and repopulating the ground state. Our current example shows that cyclopeptidic templates can be successfully used to form light-harvesting/light-converting hybrid ensembles with a distinctive organization of donor and acceptor units able to act as efficient artificial photosystems.

cyclic peptide nanotubes | fullerenes | self-assembly

Peptide-based tubular systems are being widely used to mimic Nature's channel-forming structures (1). Stable architectures ranging from β-helices to stacked macrocycles can self-assemble through multiple hydrogen-bonding interactions between and/or within peptide units with backbones capable of adopting an appropriate curvature. However, although a variety of versatile strategies have been developed to produce peptide tubes (2, 3), comparatively little has been done in the way of controlled functionalization of their inner and/or outer surfaces so as to fit them for specific tasks (4).

Peptide nanotubes (PNs) or nanotube segments formed by the self-stacking of two or more cyclic peptides (2, 3, 5) are notable examples of the "bottom-up" approach to functional nanostructures. These self-assembled PNs have found application in biological and medical research and materials science (6–10). Their self-assembly is brought about by hydrogen bonding between their constituent cyclic peptides (CPs). The chirality of the amino acid residues of the CPs is such that the CP backbone forms an essentially flat ring with its C═O and N—H groups oriented nearly perpendicular to the ring plane and its side chains radiating outward. This conformation allows each face of the CP to take part in a β-sheet-like hydrogen-bond array with another CP that, depending on the sequence of amino acid residues in the CPs, must be oriented either parallel or antiparallel to the first (11–13). Scheme 1 shows an example of the antiparallel stacking of CPs formed of alternating α- and γ-amino acid residues (α,γ-CPs). Note that the precise orientation of side chains in planes perpendicular to the CP rings depends on backbone interactions within each ring.

Within the nanobiomaterials field, one of the most actively pursued goals is the design of highly efficient and highly directional electron transfer mimics of the photosynthetic systems of plants and bacteria. In principle, self-assembled PNs bearing an appropriate array of photoactive and electroactive units might achieve this goal. Here, we describe the synthesis and physicochemical properties of a class of nanotubular cyclopeptide heterodimers in which one CP bears an electron acceptor (C_{60}), whose physico-chemical properties, its small reorganization energy in electron transfer reactions, and its ability to accept up to six electrons make this and other fullerenes attractive as potential electron-accepting units in functional assemblies and supramolecular arrays (14, 15), and the other an electron donor {2-[9-(1,3-dithiol-2-ylidene)anthracen-10(9H)-ylidene]-1,3-dithiole, exTTF} (16, 17).

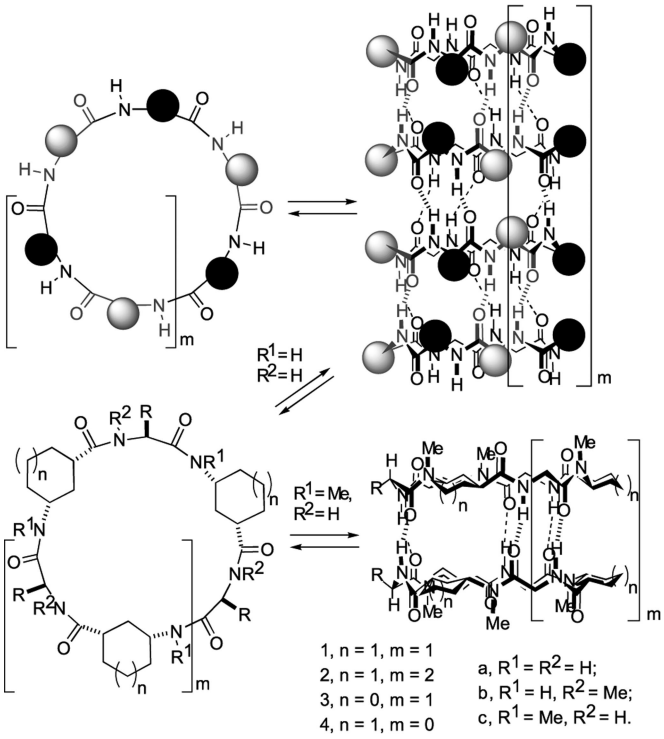

Scheme 1. Self-assembling process of CPs. (*Upper*) Self-assembled PN formation by stacking of antiparallel CPs. (*Lower*) Chemical structure of α,γ-CPs **1a–4c**, and dimeric nanotube segments formed from **1c**, **2c**, **3c**, and **4c**.

Author contributions: L.C., J.R.G., N.M., and D.M.G. designed research; R.J.B., M.A.H., L.S., and W.S. performed research; R.J.B., M.A.H., L.S., and W.S. analyzed data; and J.R.G., M.A.H., L.S., N.M., and D.M.G. wrote the paper.

The authors declare no conflict of interest.

This article is a PNAS Direct Submission.

Abbreviations: PN, peptide nanotube; CP, cyclic peptide; γ-Ach, γ-aminocyclohexanecarboxylic acid; γ-Acp, γ-aminocyclopentanecarboxylic acid; exTTF, 2-[9-(1,3-dithiol-2-ylidene)anthracen-10(9H)-ylidene]-1,3-dithiole.

†To whom correspondence may be addressed. E-mail: qojuangg@usc.es, nazmar@quim.ucm.es, or dirk.guldi@chemie.uni-erlangen.de.

This article contains supporting information online at www.pnas.org/cgi/content/full/0609506104/DC1.

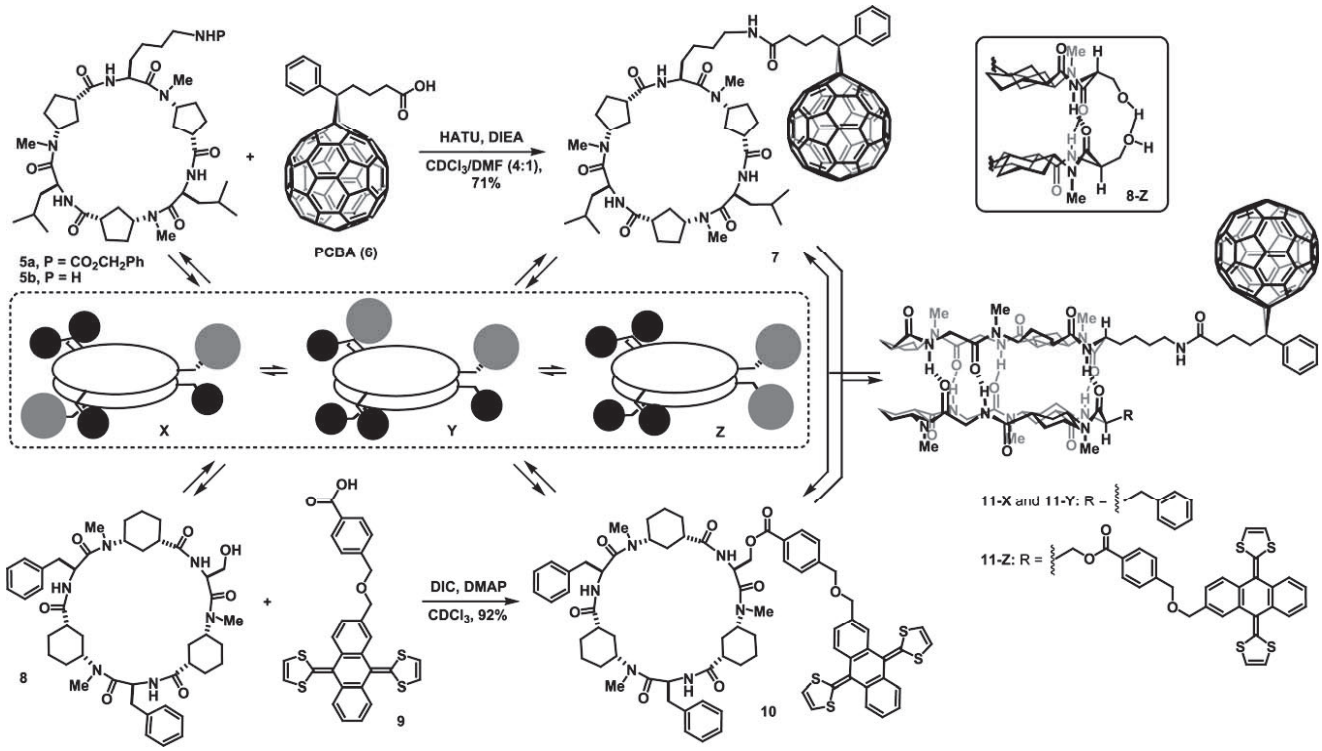

Scheme 2. Synthesis of CPs **7**–**10** and structure of heterodimer **11** are shown. Also shown is the schematic representation of the three possible registers of corresponding dimers (**X**, **Y**, **Z**) (dashed box) and hydrogen-bonding between the side chains of the serine residues of **8-Z** (solid box).

As CPs we used α,γ-CPs based on **1c** and **3c** (Scheme 1), in which the *all-trans* conformation required for CP ring flatness is ensured by the alternation of D-α-amino acids with a (1*R*,3*S*)-3-aminocycloalkanecarboxylic acid (L-γ-Aca) (18, 19). It is known that heterodimerization is particularly strong between an α,γ-CP in which the γ-amino acid is γ-aminocyclohexanecarboxylic acid (γ-Ach) and an α,γ-CP in which the γ-amino acid is γ-aminocyclopentanecarboxylic acid (γ-Acp) (20). The target heterodimer **11** is formed by the self-assembly of γ-Acp-based CP **7**, and the γ-Ach-based CP **10**, decorated with C_{60} and exTTF units, respectively. It was expected that these two CPs would dimerize to form an equilibrium mixture of three **11**-type species differing in the relative positions of their C_{60} and exTTF moieties, **11-X**, **11-Y**, and **11-Z** (Scheme 2).

The γ-Acp-based CP **7** was synthesized starting from the cyclic hexapeptide **5a**, which was obtained as described (14–16). Hydrogenation of **5a** (balloon pressure, 10% Pd/C) yielded peptide **5b**, and coupling the latter with phenyl-C61-butyric acid (PCBA) (**6**) (21) [*O*-(7-azabenzotriazol-1-yl)-1,1,3,3-tetramethyluronium hexafluorophosphate (HATU), diisopropylethylamine (DIEA), $CDCl_3$/dimethylformamide (DMF)] afforded *cyclo*[L-Lys(PCBA)-D-^{Me}*N*-γ-Acp-(L-Leu-D-^{Me}*N*-γ-Acp)$_2$] (**7**). The location of the amide proton NMR signals of **7** in nonpolar solvents (8.0–8.3 ppm) showed the formation of stable homodimers. The fact that the ^{1}H NMR spectrum remained unaltered when concentration was lowered implied a dimerization constant $>10^4$ M^{-1}, similar to those of analogous α,γ-CPs. Like **11**, homodimers of **7** can form three different dimeric species (**7-X**, **7-Y**, and **7-Z**), but the complexity of the ^{1}H NMR spectrum prevented accurate determination of their relative proportion; in this regard, whereas peptide **5a** exists as an almost equimolar mixture of **5a-X**, **5a-Y**, and **5a-Z**, peptide **8** exists as a 1:1:1.8 mixture of **8-X**, **8-Y**, and **8-Z** (see ref. 23). FTIR spectroscopy corroborated the β-sheet nature of the hydrogen-bond system mediating dimerization (22), showing bands at 1,625, 1,531, and 3,303 cm^{-1}, similar to those reported for related PNs (5, 18–20).

To prepare the exTTF-bearing CP **10** we started from the γ-Ach-based CP *cyclo*[L-Ser-D-^{Me}*N*-γ-Ach-(L-Phe-D-^{Me}*N*-γ-Ach)$_2$] (**8** in Scheme 2) (23). The esterification reaction between **8** and the exTTF derivative **9** (24) in the presence of *N*,*N*′-diisopropylcarbodiimide (DIC) and 4-dimethylaminopyridine (DMAP) afforded the desired α,γ-CP conjugate **10** in high yield (92%). The formation of three stable homodimers in $CDCl_3$ was shown by the location of six doublets at 8.6–8.8 ppm and three doublets at 8.3–8.4 ppm in the ^{1}H NMR spectrum, which also showed **10** to exist as practically equal proportions of the three possible forms, **10-X**, **10-Y**, and **10-Z**.

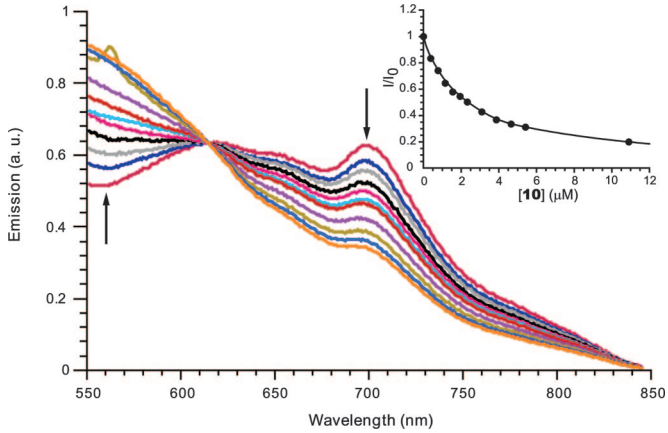

Fig. 1. Fluorescence spectral changes (λ_{exc} = 340 nm) of **7** (298 K, dichloromethane, 4.4×10^{-6} M) upon addition of different amounts of **10** (0, 0.44, 0.88, 1.32, 1.76, 2.20, 2.64, 3.08, 3.52, 4.40, 5.28, and 10.56×10^{-6} M). (*Inset*) Displayed is the relationship of I/I_0 versus **10** that was used to determine the association constant.

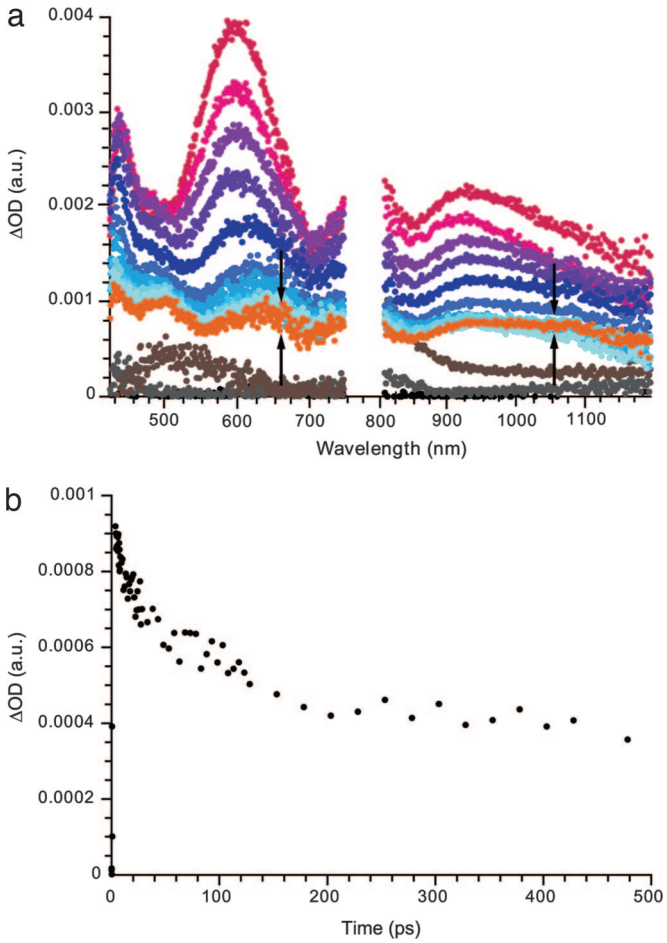

Fig. 2. Femtosecond flash photolysis of heterodimer **11**. (*a*) Differential absorption spectra (visible and NIR) obtained upon femtosecond flash photolysis (387 nm) of heterodimer 11 (≈5.0 μM) in nitrogen-saturated dichloromethane with several time delays between 0 and 200 ps at room temperature. Arrows indicate the features of the radical ion pair state. (*b*) Time-absorption profiles of the spectra shown in *a* at 660 nm, monitoring the intrahybrid charge separation process.

Addition of 1 eq of **10** to a 2 mM solution of **7** in $CDCl_3$ afforded all three forms of heterodimer **11**; their amide proton NMR signals appear at 8.1–8.7 ppm [supporting information (SI) Fig. 5]. The ^{1}H NMR spectra of similar mixtures of **7** and **10** were unchanged by dilution down to 2×10^{-4} M, heating to

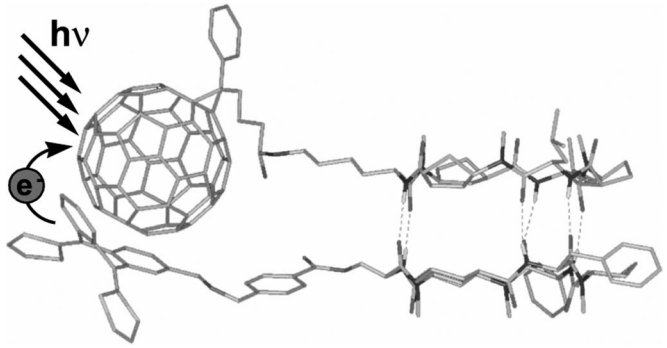

Fig. 3. Computer-generated structure of heterodimer **11-Z**, showing photoinduced electron transfer facilitated by the proximity of the donor and acceptor units (exTTF and C_{60}, respectively).

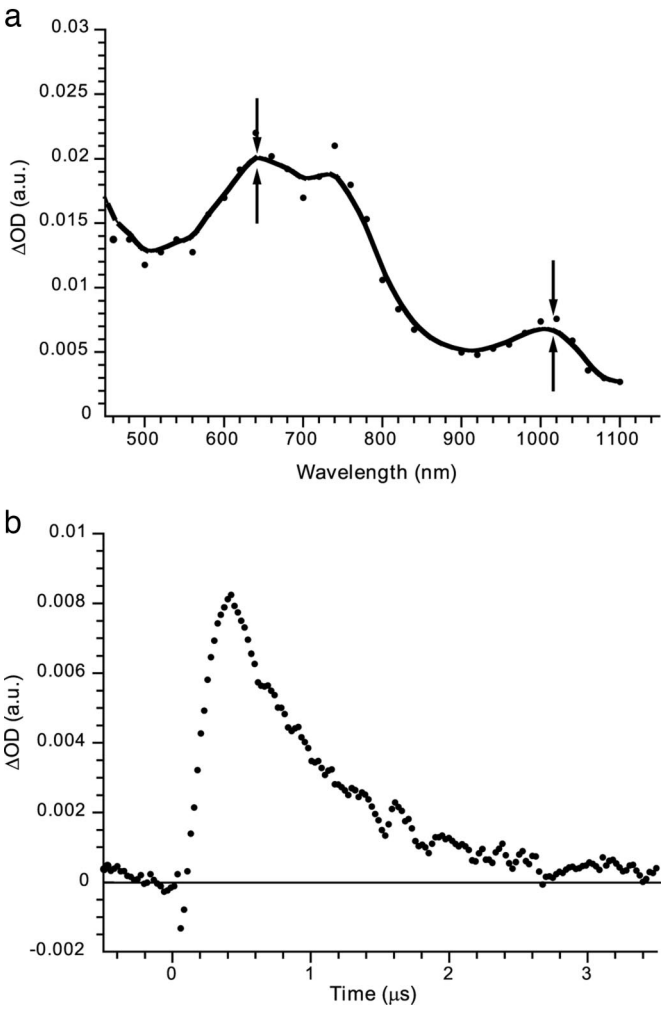

Fig. 4. Nanosecond flash photolysis of heterodimer **11**. (*a*) Differential absorption spectrum (visible and NIR) obtained upon nanosecond flash photolysis (355 nm) of heterodimer 11 (≈5.0 μM) in nitrogen-saturated dichloromethane with a 50-ns time delay at room temperature. Arrows indicate the features of the radical ion pair state. (*b*) Time-absorption profiles of the spectrum shown in *a* at 1,040 nm, monitoring the charge recombination process.

323 K, or addition of methanol, which implies a high affinity for these dimeric complexes. Although the complexity of the ^{1}H NMR spectrum of **11** prevented accurate determination of the relative proportions of **11-X**, **11-Y**, and **11-Z**, it is thought that, just as homodimer **8-Z** is formed to a greater extent than **8-X** and **8-Y** because of hydrogen bonding between favorably oriented serine hydroxy groups (Scheme 2), van der Waals interactions between the C_{60} and exTTF units of **11-Z** could facilitate the formation of this isomer in preference to **11-X** and **11-Y**, and through-space electron transfer (25).

Fig. 1 shows fluorescence spectra of a solution of **7** in dichloromethane that were recorded after addition of increasing amounts of **10**. The fullerene characteristic peak at 700 nm is quenched upon dimerization, and the dependence of fluorescence intensity on the concentration of **10** implies an association constant of at least 10^6 M^{-1}.

The electrochemical properties of **7**, **10**, and **11** were investigated at room temperature by cyclic voltammetry and differential pulse voltammetry (SI Table 1 and SI Fig. 6). The redox behavior of the electroactive groups of homodimers of **7** and **10** (C_{60} and exTTF) is largely preserved in heterodimer **11** (16, 17,

26), but oxidative scans of **11** nevertheless show a shift of approximately +50 mV relative to those of the exTTF/exTTF^{2+} couple of homodimers of **10**. This shift may be a consequence of a weak intramolecular electronic interaction between the exTTF moiety and the fullerene-based peptide in the ground state.

The above evidence of donor–acceptor interaction between the photo and redox active side chains of **11** (see Fig. 1) was corroborated by time-resolved transient absorption measurements in which the fullerene moiety was photoexcited at 387 nm by 150-fs laser pulses. Whereas the spectra of homodimers of **7** exhibited the characteristic transient fluorescence maximum at ≈900 nm (SI Fig. 7) correponding to the singlet excited state of fullerene, followed by a slow transition to a transient maximum at 720 nm corresponding to the triplet state, the spectra of **11** demonstrated that the fullerene singlet excited state decays very fast (i.e., 0.055 ns) and forms the radical ion pair state, $C_{60}^{\bullet -}$/exTTF$^{\bullet +}$. The spectral characteristics observed at 680 and 1,040 nm resemble the fingerprints of the one-electron oxidized exTTF (i.e., exTTF$^{\bullet +}$) and the one-electron reduced fullerene (i.e., $C_{60}^{\bullet -}$), respectively (Fig. 2) (27–30). On the time scale of up to 1,600 ps, no notable decay of the radical ion pair state features is observed, which rules out a fast intrahybrid charge recombination. In fact, charge separation caused by photoexcitation of exTTF in either heterodimer **11** or homodimers of **10** is negligible, and an efficient electron transfer is precluded by the short lifetime (≈0.86 ps) of the transient species with a spectral peak at 605 nm (SI Fig. 8) (31).

The above charge separation process is presumably limited to heterodimer **11-Z** (Fig. 3), because the distances between C_{60} and exTTF in **11-X** and **11-Y** (>15 Å) are unlikely to power an intrahybrid electron transfer reaction. However, these latter isomers appear to undergo singlet-to-triplet processes on a time scale similar to that of homodimers of **7** (τ = 1.4 ns). This hypothesis is supported by fluorescence lifetime measurements of **11**, which show an ≈1:2 ratio of two processes with lifetimes of <0.1 and ≈1.5 ns, respectively.

The formation of two distinct photoproducts was corroborated by the results of nanosecond-scale experiments in which charge recombination was investigated after photoexcitation of heterodimer **11** at 355 nm. The transient spectra obtained in these experiments (Fig. 4*a*) show features at ≈360 and 720 nm that are attributable to the triplet excited state of fullerene, which presumably correspond to **11-X** and **11-Y**, and peak at 660 and 1,040 nm that are attributed to exTTF$^{\bullet +}$ and $C_{60}^{\bullet -}$, respectively. The decay profiles of these spectra imply lifetimes of 25 μs for the triplet state (which decays to the singlet ground state) and 0.86 μs for the radical ion pair state.

In conclusion, we have prepared a bio-inspired nanohybrid, **11**, in which a CP bearing an electron-donor unit (exTTF) is coupled by a β-sheet-like hydrogen-bond system to another bearing a photoactive electron-acceptor unit (C_{60}). Photoexcitation of the fullerene chromophores to their 1.76-eV excited state is followed, in one of the three forms of **11**, by a charge separation process generating a 1.15-eV radical ion pair state. On average, this state perdures for at least 1.5 μs, which is comparable to the performance of other noncovalent C_{60}-based hybrids (in which electron transfer occurs basically via through-space interactions) (14, 15, 31–33) and is superior to that of typical covalent C_{60}–exTTF conjugates (25–28). The structure of **11** in principle allows its extension to form a nanotubular battery along which electron donors and electron acceptors alternate and also suggests the possibility of designing molecular switches based on dynamic control of interconversion between the electroactive isomer **11-Z** and the inactive isomers **11-X** and **11-Y**.

Detailed descriptions of the synthesis and characterization of key compounds, including NMR spectra (^{1}H and ^{13}C, NOESY and/or ROESY) and FTIR spectra of peptides **5a**, **7**, **10**, and **11**; electrochemical data for compounds **7**, **10**, and **11**; and differential absorption spectra are available in *NMR Spectra* in *SI Text*.

This work was supported by the Ministry of Education and Science of Spain under Projects SAF2004-01044 (jointly with the European Regional Development Fund), CTQ2005-02609/BQU, and P-PPQ-000225-0505; the Xunta de Galicia under Project PGIDT04BTF209006PR; SFB583, DFG (60517/4-1), Fonds der Chemischen Industrie, and the Office of Basic Energy Sciences of the U.S. Department of Energy under Notre Dame Radiation Laboratory Project NDRL 4715; an Formación de Profesorado Universitario grant from the Ministry of Education and Science of Spain (to R.J.B.); and a Ramón y Cajal contract from the Ministry of Education and Science of Spain (to M.A.H.).

1. Ghadiri MR, Granja JR, Buehler LK (1994) *Nature* 369:301–304.
2. Brea RJ, Granja JR (2004) in *Dekker Encyclopedia of Nanoscience and Nanotechnology*, eds Schwarz JA, Contescu CI, Putyera K (Dekker, New York), pp 3439–3457.
3. Bong DT, Clark TD, Granja JR, Ghadiri MR (2001) *Angew Chem Int Ed* 40:988–1011.
4. Balbo Block MA, Hecht S (2005) *Angew Chem Int Ed* 44:6986–6989.
5. Clark TD, Buriak JM, Kobayashi K, Isler MP, McRee DE, Ghadiri MR (1998) *J Am Chem Soc* 120:8949–8962.
6. Martin CR, Kohli P (2003) *Nat Rev* 2:29–37.
7. Gao X, Matsui H (2005) *Adv Mater* 17:2037–2050.
8. Ghadiri MR, Granja JR, Buehler LK (1994) *Nature* 369:301–304.
9. Sánchez-Quesada J, Kim HS, Ghadiri MR (2001) *Angew Chem Int Ed* 40:2503–2506.
10. Fernández-López S, Kim HS, Choi EC, Delgado M, Granja JR, Khasanov A, Kraehenbuehl K, Long G, Weinberger DA, Wilcoxen K, Ghadiri MR (2001) *Nature* 412:452–455.
11. Vollmer MS, Clark TD, Steinem C, Ghadiri MR (1999) *Angew Chem Int Ed* 38:1598–1601.
12. Couet J, Samuel JDJS, Kopyshev A, Santer S, Biesalski M (2005) *Angew Chem Int Ed* 44:3297–3301.
13. Horne WS, Ashkenasy N, Ghadiri MR (2005) *Chem Eur J* 11:1137–1144.
14. Guldi DM, Rahman GMA, Ehli C, Sgobba V (2006) *Chem Soc Rev* 35:471–487.
15. Martín N (2006) *Chem Commun*, 2093–2104.
16. Yamashita Y, Kobayashi Y, Miyashi T (1989) *Angew Chem Int Ed Engl* 28:1052–1053.
17. Bryce MR, Moore AJ, Hasan M, Ashwell GJ, Fraser AT, Clegg W, Hursthouse MB, Karaulov AI (1990) *Angew Chem Int Ed Engl* 29:1450–1452.
18. Amorín M, Castedo L, Granja JR (2003) *J Am Chem Soc* 125:2844–2845.
19. Amorín M, Castedo L, Granja JR (2005) *Chem Eur J* 11:6543–6551.
20. Brea RJ, Amorín M, Castedo L, Granja JR (2005) *Angew Chem Int Ed* 44:5710–5713.
21. Hummelen JC, Knight BW, Le Peq F, Wudl F, Yao J, Wilkins CL (1995) *J Org Chem* 60:532–538.
22. Haris PI, Chapman D (1995) *Biopolymers (Peptide Sci)* 37:251–263.
23. Amorín M, Villaverde V, Castedo L, Granja JR (2005) *J Drug Del Sci Tech* 15:87–92.
24. Herranz MA, Martín N, Campidelli S, Prato M, Brehm G, Guldi DM (2006) *Angew Chem Int Ed* 45:4478–4482.
25. Pérez EM, Sánchez L, Fernández G, Martín N (2006) *J Am Chem Soc* 128:7172–7173.
26. Echegoyen LE, Herranz MA, Echegoyen L (2006) in *Encyclopedia of Electrochemistry*, eds Bard AJ, Stratmann M, Scholz F, Pickett CJ (Wiley, Weinheim, Germany), Vol 7, pp 145–201.
27. Martín N, Sánchez L, Guldi DM (2000) *Chem Commun*, 113–114.
28. Díaz MC, Herranz MA, Illescas BM, Martín N, Godbert N, Bryce MR, Luo C, Swartz A, Anderson G, Guldi DM (2003) *J Org Chem* 68:7711–7721.
29. Giacalone G, Segura JL, Martín N, Guldi DM (2004) *J Am Chem Soc* 126:5340–5341.
30. Sánchez L, Sierra M, Martín N, Guldi DM, Wienk MM, Janssen RAJ (2005) *Org Lett* 7:1691–1694.
31. Sánchez L, Sierra M, Martín N, Myles AJ, Dale TJ, Rebek J, Jr, Seitz W, Guldi DM (2006) *Angew Chem Int Ed* 45:4637–4641.
32. Sessler JL, Jayawickramarajah J, Gouloumis A, Torres T, Guldi DM, Maldonado S, Stevenson KJ (2005) *Chem Commun*, 1892–1894.
33. McClenaghan ND, Grote Z, Darriet K, Zimine M, Williams RM, De Cola L, Bassani DM (2005) *Org Lett* 7:807–810.